SAND2023-05881C

METHODOLOGY FOR CONSEQUENCE-BASED SETBACK DISTANCE CALCULATIONS FOR BULK LIQUID HYDROGEN STORAGE SYSTEMS

Hecht, E.S.[a], Ehrhart, B.D.[b], and Schroeder, B.B.[b]

[a]**Hydrogen and Materials Science, Sandia National Laboratories, P.O. Box 969, MS 9052, Livermore, CA 94551, USA, ehecht@sandia.gov**

[b]**Risk & Reliability Analyses, Sandia National Laboratories, P.O. Box 5800, MS 0748, Albuquerque, NM 87185, USA, bdehrha@sandia.gov, bbschro@sandia.gov**

ABSTRACT

Updates to the separation distances between different exposures and bulk liquid hydrogen systems are included in the 2023 version of NFPA 2: Hydrogen Technologies Code. This work details the models and calculations leading to those distances. The specific models used, including the flow of liquid hydrogen through an orifice, within the Hydrogen Plus Other Alternative Fuels Risk Assessment Models (HyRAM+) toolkit, are described and discussed to emphasize challenges specific to liquid hydrogen systems. Potential hazards and harm affecting individual exposures (e.g., ignition sources, air intakes) for different unignited concentrations, overpressures, and heat flux levels were considered, and exposures were grouped into three bins. For each group, the distances to a specific hazard criteria (e.g., heat flux level) for a characteristic leak size, informed by a risk-analysis, led to a hazard distance. The maximum hazard distance within each group was selected to determine a table of separation distances based on internal pressure and pipe size, rather than storage volume, similar to the bulk gaseous separation distance tables in NFPA 2. The new separation distances are compared to the previous distances, and some implications of the updated distances are given.

1.0 INTRODUCTION

In the United States, the National Fire Protection Association's Hydrogen Technologies Code (NFPA 2) has been adopted by many jurisdictions [1]. Language around how hydrogen components (both gaseous and liquid) should be arranged on a site is included in NFPA 2. While the final decision rests with the authority having jurisdiction (typically the fire marshal), there are prescriptive distances between bulk storage systems (both gaseous and liquid) and different exposures (e.g., building openings, lot lines, other flammables). We note that separation distances are meant to protect against common leak scenarios (which are likely to be small) and other engineering controls are necessary to protect against worst case scenarios (e.g., sufficient overpressure relief systems are necessary to prevent a boiling liquid expanding vapor explosion). The distances between bulk liquid hydrogen storage systems and exposures remained unchanged and served industry well since their introduction in the 1967 edition of NFPA 50B (which was later incorporated into NFPA 55 and then to NFPA 2), but the specific basis for those distances has been lost to history. In addition, practical knowledge of use and updated modeling tools presented an opportunity to develop new, science-based distances in the 2023 edition of NFPA 2 [1]. This work describes the modeling and calculations that led to those distances.

Previous work by an NFPA storage task group led to risk-informed separation distances for bulk gaseous hydrogen systems in the 2011 version of NFPA 2 [2, 3]. Quantitative risk assessment was used to determine a characteristic leak size from gaseous hydrogen systems, and deterministic physical modeling of a flame and dispersion was used to calculate the separation distances. In addition, this task group concluded that the pressure and leak size were the determining

characteristics of the system for separation distances, as the volume would affect duration, but not the hazard level at a given distance (the hazard level would likely even decrease as the tank pressure decreased). For modification of the bulk liquid separation distances in the 2023 edition of NFPA 2, the task group came to similar conclusions: risk analyses could be used to determine a characteristic leak size, and the separation distances should be based on pressure and leak size rather than volume of the system.

The risk-basis to determine the characteristic leak size for consequence-based analyses are described in another work at this conference [4], as well as in Ehrhart et al. [5]. The conclusion is that a 5% leak size (based on the internal flow area of interconnecting piping) is a conservative but reasonable assumption. Because a specific liquid hydrogen system will have a unique design for the flow system, similar to the bulk gaseous hydrogen separation distances, the bulk liquid hydrogen separation distances in this work are calculated for a range of characteristic pipe sizes and tables were developed to select the separation distance for a specific system (i.e., the tables show the separation distances as a function of pipe size). The task group also noted that a range of storage pressures may be used for liquid hydrogen systems and calculations for different pressures were also made. Hydrogen can be a liquid only up to its critical pressure of 13.0 bar_a (188 psi_a), which was used as the maximum pressure.

This paper describes the consequence based modeling that resulted in the updated science-based bulk liquid hydrogen storage tank separation distances in the 2023 edition of NFPA 2 [1]. First, the models in HyRAM+ version 4.1 [6] are compared to literature data for liquid hydrogen experiments. Then the calculation of the distances for each of the criteria for each of the groups are described along with the generation of the separation distance tables. Finally, the new distances are compared to the previous values to help assess the impact of the latest bulk liquid hydrogen storage separation distances.

2.0 APPROACH

The NFPA 2 task committee recommended that changes to the liquid hydrogen setback distances be well-documented, retrievable, repeatable, revisable, independently-verified, and used experimental results to verify and validate behavior models. In order to make the work repeatable and revisable, all of the calculations were made with version 4.1 of the Hydrogen Plus Other Alternative Fuels Risk Assessment Models (HyRAM+) [6]. HyRAM+ is an open source software toolkit with a graphical user interface for Windows machines that can be downloaded from `https://hyram.sandia.gov`; the Python based back-end can also be installed independently from the Python Packaging Index (`https://pypi.org/project/hyram/`) or Anaconda's conda-forge (`https://anaconda.org/conda-forge/hyram`). The models in HyRAM+ 4.1 are documented in a technical reference manual [7]. For the necessary calculations in this work, the Python back-end of HyRAM+ version 4.1.1 was used; the Windows GUI does not have the flexibility to make all of the calculations.

While some of the models have been validated in HyRAM+ for hydrogen [8] (and methane and propane [9]), previous comparisons were limited to cold gaseous hydrogen (near liquid temperatures) rather than liquid hydrogen releases. This effort therefore began by comparing the HyRAM+ results to data for liquid hydrogen. As shown below, there was a very limited set of data that was found, but nonetheless, the models were compared to data for each of the quantities of interest for the models needed to develop the updated separation distances. This includes flow through an orifice, unignited dispersion, radiative heat flux from flames, and overpressure from the delayed ignition of an unconfined release.

Harm criteria is also a necessary benchmark for determining separation distances. Hazards associated with liquid hydrogen are similar to gaseous hydrogen, primarily stemming from its flammability. A small leak will generally flash to vapor due to heat in the air before even coming in contact with a surface [10–12]. While contact with cold can cause harm, it was not considered a primary hazard in this analysis. Similar to the harm criteria for bulk gaseous hydrogen

Table 1. Exposure groups and harm criteria.

Exposure	Criteria
Group 1	
1. Lot lines 2. Air intakes (e.g. HVAC, compressors) 3. Operable openings in buildings and structures 4. Ignition sources such as open flames and welding	• Average mole fraction of 8% • Heat flux of 4.732 kW/m^2 • Peak overpressure of 6.9 kPa
Group 2	
5. Exposed persons other than those servicing the system 6. Parked cars 7. Buildings of combustible construction 8. Hazardous materials storage systems above ground or fill/vent openings for below ground storage systems 9. Ordinary combustibles, including fast-burning solids such as ordinary lumber, excelsior, paper, or combustible waste and vegetation other than that found in maintained landscaped areas	• Heat flux of 9 kW/m^2 • Peak overpressure of 13.8 kPa
Group 3	
10. Buildings of noncombustible non-fire-rated construction 11. Flammable gas storage systems above or below ground 12. Heavy timber, coal, or other slow-burning combustible solids 13. Unopenable openings in buildings and structures 14. Encroachment by overhead utilities (horizontal distance from the vertical plane below the nearest overhead electrical wire of building service) 15. Piping containing other hazardous materials 16. Flammable gas metering and regulating stations such as natural gas or propane	• Heat flux of 20 kW/m^2 • Visible flame length • Peak overpressure of 20.7 kPa

systems, the storage task group considered the distance to a specific unignited concentration or heat flux level from a flame in this analysis, and as an additional criteria to gaseous hydrogen also considered the overpressure from the delayed ignition of a leak. Exposures themselves were also regrouped by the task group. Details of the grouping and reasoning behind the criteria are given in Ehrhart et al. [5]; a summary is provided in Table 1.

With a characteristic leak size, validated models and harm criteria, calculation of the setback distances is straightforward. For a specific pressure and pipe size, each of the models was run to generate the distance to the criteria, and within a group, the criteria with the maximum distance was selected. Pressures were divided into three potential operating ranges: $P_g \leq 414$ kPa, $414 < P_g \leq 827$ kPa, and $827 < P_g \leq 1200$ kPa. As shown below (see Fig. 1 in Section 3.1), the maximum mass flow rate for liquid hydrogen between 827 and 1200 kPa does not occur at the critical pressure (1200 kPa), but rather at 1090 kPa. This is because the speed of sound (which is lower for liquid than gas) for the two-phase mixture at the orifice decreases at a rate less than the density increases as the critical pressure is approached. As the largest flame or plume will be generated at the maximum mass flow rate rather than the maximum pressure, for the highest pressure bin, 1090 kPa was therefore used as the pressure for the calculations. For the lower two bins, the maximum pressure within the range (414 and 827 kPa) were used as the pressures in the calculations, as these are the pressures that cause the maximum flow rate within these bins.

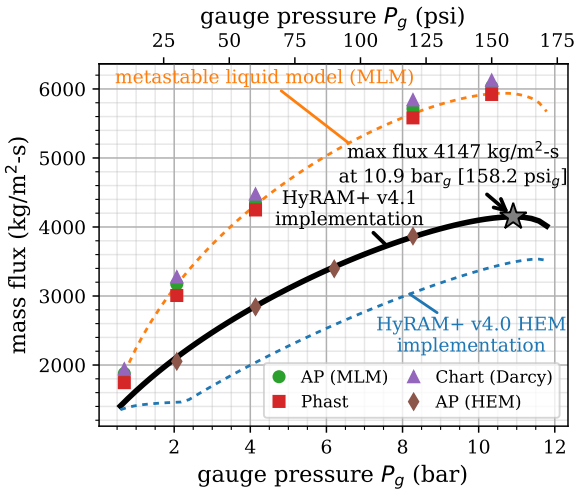

Figure 1. Calculations of mass flux for implementations of MLM and HEM models.

3.0 RESULTS AND DISCUSSION

3.1 Orifice Flow

The first step in a liquid hydrogen release is the flow through an orifice. In order to calculate this flow, the state of the fluid upstream of the leak must be defined by two thermodynamic properties, typically pressure and phase (i.e., subcooled liquid at a specified temperature, saturated liquid, two-phase with a specific liquid/vapor fraction, or saturated vapor). For a cryogenic fluid, there are then several modeling assumptions that could be made to calculate the flow through an orifice. Two that were considered were a metastable liquid model (MLM) and a homogeneous equilibrium model (HEM). The MLM assumes that a liquid upstream of a leak will remain a liquid at constant density as it flows through the leak. This results in high density liquid flowing through the orifice (rather than a lower density two-phase mixture) resulting in predictions of high mass flowrates.

The HEM on the other hand (in the HyRAM+ implementation) assumes that the fluid flowing through the orifice remains isentropic. In most cases, this means that a saturated liquid (or even slightly subcooled liquid) will flash to a lower density two-phase mixture at the throat resulting in lower flowrates than the MLM. The gas and fluid phases are assumed to flow at the same velocity (homogeneously) through the throat. Previous versions of HyRAM+ (< 4.1) used a HEM to calculate flow through an orifice but relied on a calculation of the speed of sound of the two-phase mixture that formed in the throat as a saturated liquid flashed to two-phase. This calculation is uncertain, as there are challenges in measuring the speed of sound of two-phase flows, especially for cryogenic fluids. Rather than calculating the two-phase speed of sound, HyRAM+ version 4.1 solves for the maximum mass flux through an orifice as the fluid pressure drops isentropically while flowing through an orifice [7]. This calculation method results in the speed of sound for single-phase fluids (and therefore this method is also suitable for gas flows), and relies only on the enthalpy and entropy of the two-phase mixture, a much more reliable calculation than the two-phase speed of sound.

The considered flow models were first verified against other implementations by Air Products, Chart Industries, and PHAST. This comparison can be seen in Fig. 1. As shown, the previous calculation that relied on the speed of sound of a two-phase mixture (dashed blue line) underpredicted the mass flux relative to the current implementation of the HEM. Both the Air Products implementation and the HyRAM+ implementation result in the same mass flux. The MLM predicts much higher mass fluxes than the HEM. The mass fluxes predicted using the MLM were reproduced by Chart Industries and Air Products. The MLM and HEM models

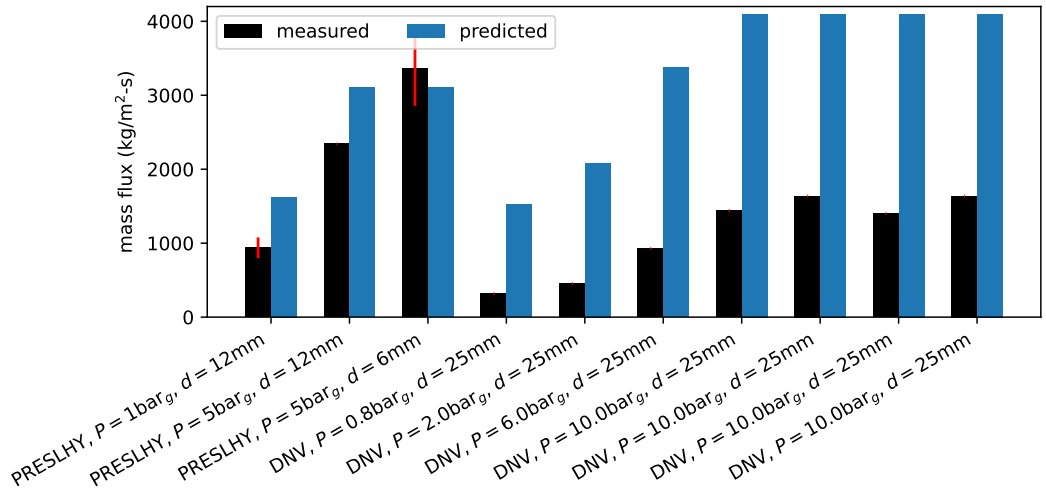

Figure 2. Mass fluxes for experiments (PRESLHY [11] and DNV [12]) compared to predictions. Red lines indicate estimated 15% error on some experiments due to gas bubbles.

were compared to experimental data (detailed below) and the MLM model significantly over-predicted the measured flowrates. Because the orifice flowrates were more accurately predicted (or more modestly overpredicted) by the HEM model and this is the same calculation as is used for compressed gaseous flows, the HEM model (with the new maximum mass flux search algorithm) was selected as the flow model in HyRAM+ [7].

Two experimental campaigns, by DNV-GL [12], and by the Health and Safety Executive under the Prenormative Research for Safe Use of Liquid Hydrogen (PRESLHY) project [11], measured the mass flows of liquid hydrogen while performing experiments. These experiments featured several measures of pressure in the tank upstream of the release and just before the release point. The test data is shown as the black bars. The flows predicted in HyRAM+ 4.1, using the tank pressure (as is used in calculation of the separation distances), are shown as the blue bars in Fig. 2. With the exception of the 5 bar (500 kPa), 6 mm PRESLHY experiment, the mass flux is overpredicted by HyRAM+. In this case, the authors [11] show some unsteadiness in the mass flow rate measurements, which they presume was caused by gas bubbles disturbing the measurement, with 10-20% error, as indicated by the red line (15% error is shown here) at the top of the data bar. Using the tank pressure and the HEM is generally conservative as compared to test data. Using HEM model and storage tank pressure to model a leak rate is additionally conservative since a real system will have piping, which introduces pressure loss and therefore the pressure at the release point will not be as high as the pressure in the tank.

The dispersion and flame models are one-dimensional integral models where the boundary conditions are specified for atmospheric pressure gaseous rather than above ambient pressure, liquid, or two-phase flows. After flowing through the orifice, the fluid is assumed to continue with the same mass, momentum, and energy until it reaches atmospheric pressure (i.e., the notional nozzle model described by Yüceil and Ötügen [13]), begins to entrain air, and flashes to a gas, neglecting any effects from air or humidity condensation as described by Hecht et al. [7].

3.2 Unignited Dispersion

There were two horizontal releases during the DNV-GL experimental campaign [12], which were repeats of the same experiment. These were both 10 bar tank pressure releases through a 25.4 mm nozzle. Measurements of concentration using oxygen sensors were made at several heights from 0.1–1.8 m above the ground at 30, 50, and 100 m from the nozzle. The maximum concentration at any height at these three radii are shown in Fig. 3. There were significant variations in the maximum concentration at different times, owing to the unsteadiness of the

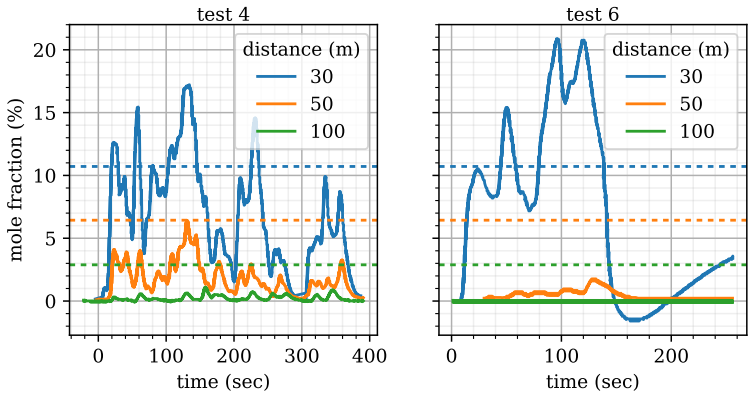

Figure 3. Experimental data of observed concentration (solid lines) [12] compared to HyRAM+ predictions (dashed lines) at several distances from a horizontal release of LH2.

Table 2. Measured maximum and calculated average concentrations in the far-field for the PRESLHY experiments [11]

Nozzle diameter [mm]	Tank pressure [barg]	Measured concentration [vol-%]	HyRAM+ concentration at (14 m, 1.5 m) [vol-%]	HyRAM+ streamline concentration at 14 m [vol-%]
25.4	1	> 4	20.7	20.9
12	1	> 4	9.7	11.0
6	1	2.15	1.1	5.6
25.4	5	> 4	18.8	20.5
12	5	> 4	10.2	10.7
6	5	3.32	5.6	5.6

wind (6.7 m/s average, 12.1 m/s max for test 4 and 2.7 m/s average, 5.8 m/s max for test 6). For these releases, the concentration dropped below the lower flammability limit somewhere between 50 and 100 m. Test 6 was ignited at about 140 sec, the time at which the mole fractions drop to zero or erroneously read below zero. The HyRAM+ predicted concentrations along the streamline (not at a specific height, and neglecting the effects of wind), shown by the horizontal dashed lines, are lower than the maximum concentration measurements at 30 m for some times throughout the test, but in the far field at 50 and 100 m predicted concentrations are above or equal to those observed. Wind was neglected in these calculations and the predictions are expected to be conservative because the distance along the streamline is used (rather than a bird-eye distance to a concentration level) and regardless of direction, wind has been shown to improve mixing and reduce the average concentration of a plume [14].

The PRESLHY campaign [11] had several measures of unignited concentrations, in both the near-field and the far-field. The far-field data is more relevant to the distance calculations because distances to low concentration values rather than high values are of interest. In the far-field, a sensor was placed 14 m from the releases at a height of 1.5 m. The sensor could measure concentrations up to the lower flammability limit (4%). In this work, for distance calculations to the different harm criteria, the streamline distance to a given concentration is used. Therefore, when comparing to the test data, the concentration predicted by HyRAM+ exactly at the point (14 m, 1.5 m), as well as 14 m along the streamline is presented. In this way, the measured concentrations, which had wind influencing their measurements can be compared to the conservative estimates of distance used to calculate setback distances in this work. The concentrations are compared to the data in Table 2. Buoyancy is evident in the HyRAM+ predictions because the concentrations along the streamline at 14 m are all greater than the concentrations at the point (14 m, 1.5 m). For the two quantitative points from the 6 mm nozzle, the concentration is slightly underpredicted for the 1 bar release at the

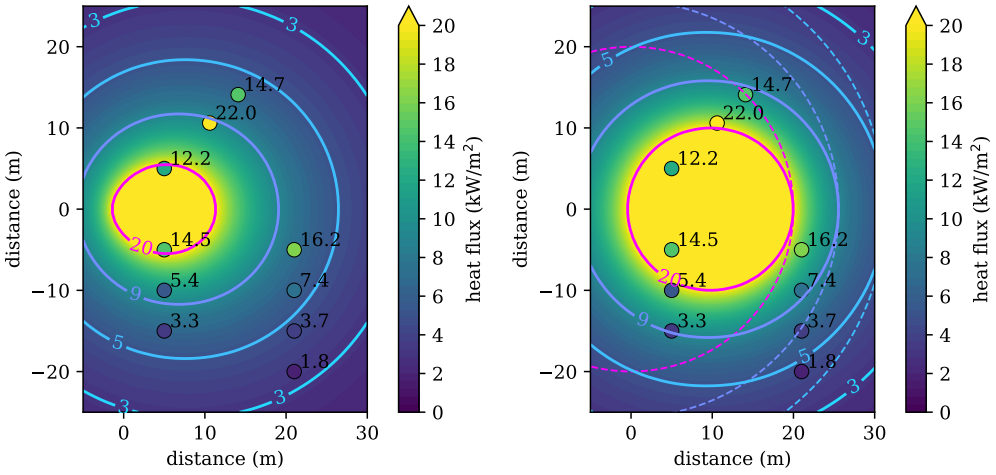

(a) At sensor height (1.2 m).

(b) Bird's-eye view.

Figure 4. HyRAM+ heat flux predictions (shading and solid contour lines) vs data (points) for the DNV-GL test 6 flame [12]. Dashed lines are circular around the leak point passing through the maximum extent of the criteria (i.e., the setback distance).

measurement point, and overpredicted for the 5 bar release. The streamline predictions are both higher than the measurements. The accuracy of the predictions is likely affected by the wind in the experiments, which ranged from 1.8–3.5 m/s, generally in-line with the releases, which could blow a brief pocket of high concentration fluid past the sensors and increase the observed maximum concentration. In general, wind in any direction will reduce the average concentration of a plume [15].

3.3 Jet Flame Length and Heat Flux

As described by Hecht and Ehrhart [7], the flame length in HyRAM+ is calculated based on a correlation described by Houf and Schefer [16], with the trajectory calculated using the model described by Ekoto et al. [17]. We were unable to find any data on flame length for liquid hydrogen flames, but the model agreed well with gaseous cryogenic lab-scale flames, as documented by Ehrhart et al. [8]. The flame length and trajectory are subsequently used in the heat flux calculation, so validation of the heat flux prediction is an indication of the flame model accuracy.

There was a single ignited horizontal release during the DNV-GL experimental campaign, test 6 [12] for which heat flux data was reported. This was a 10 bar tank pressure release through a 25 mm orifice at a height of 0.49 m. The wind was around 3 m/s nominally in the direction of the release/flame. Radiometers at several locations measured the heat flux from the flame. Figure 4 shows the measured heat fluxes as points and predicted heat flux for an ignited release (jet flame) of 10 bar, saturated liquid hydrogen through a 25 mm orifice at a height of 0.49 m with a 3 m/s wind blowing in the same direction as the flow. Figure 4a shows the heat fluxes at the height of the measurements, 1.2m, while Fig. 4b shows the 'birds-eye' heat flux that is used for setback distance calculations in this work. The 10 points are at the locations of the radiometers and are colored and labeled by the average value of the measurements. The measurements show the highest heat flux at a location of (10 m, 10 m); the wind is likely blowing the flame in the positive y-direction. The 3 m/s wind in the modeling (accessed by using the Python back-end of HyRAM+ [7]) does not capture this angle, as the wind is assumed to be directly inline with the release direction. Wind in the model only affects the x-momentum of the flame, causing it to appear to have less buoyancy and remain closer to the ground. HyRAM+ tends to underpredict the highest measured heat fluxes and overpredict the smallest heat fluxes. Focusing on the right-hand frame (Fig. 4b, the distance from the origin to the x-value of the

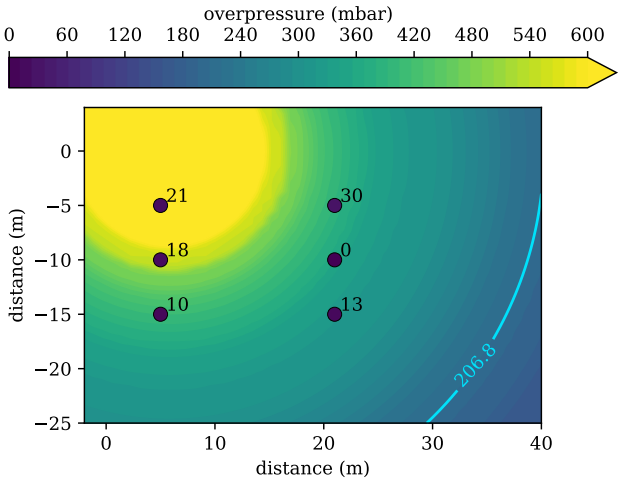

Figure 5. Peak overpressures observed after ignition of DNV-GL's test 6 (points) [12] as well as those predicted by HyRAM+ (shading and contour line).

birds-eye heat flux contours of interest for setback distances (20, 9, and 4.7 kW/m^2) are each further than the distance from the origin to the measured heat fluxes (i.e., a higher heat flux measurement is never found outside the respective dashed circle).

3.4 Unconfined Overpressure

Pressure sensors were also present for the horizontal, ignited release during the DNV-GL experimental campaign, test 6 [12]. At the time of ignition, all of the pressure sensors peaked for about 0.1 seconds. One sensor reached 30 mbar while the others peaked about 10-20 mbar. The peak observed overpressures, as well as those overpressures predicted by HyRAM+ are shown in Fig. 5. The HyRAM+ predictions use the Baker-Strehlow-Tang (BST) method as described in Hecht and Ehrhart [7], with modifications suggested by Jallais et al. [18] of using the flammable mass from 10-75%, and a Mach flame speed based on the mass flow rate (0.7 for this test). This is the same calculation as would be made during setback distance calculation. HyRAM+ vastly overpredicts the overpressures in this case. For context, the 207 mbar (3 psi) contour is also shown on the plot. This is the overpressure-based setback distance for Group 3 hazards (as shown in Table 1).

3.5 Setback Distances

The verified and validated models were used to calculate distances for a 5% by area leak to the criteria shown in Table 1. For the distance to an 8% mole fraction, the curved, streamline distance to that concentration was calculated. This distance is slightly longer than the horizontal projection of the unignited concentration, owing to the buoyancy of the ungnited plumes. For example, for the lowest pressure release (414 kPa), the 8% mole fraction contour and the streamline trajectory of the release are shown in Fig. 6a. The streamline trajectory is 0.3% longer than the horizontal projection of the distance to the 8% mole fraction, but this difference may be larger for other release pressures and orifice sizes. For the heat flux and visible flame length calculations, a 5 m/s wind along the release direction was included in the calculation to reduce the buoyancy of the flame. Owing to the high temperatures (and corresponding low density) of the products of the flames, the predicted buoyancy of the flames was high. An example calculation of a flame is shown in Fig. 6b, with the dashed line showing the predicted trajectory without a cross-wind. The cross-wind, which is a term only on the x-momentum equation and does not affect the mixing or cooling [7], causes the flame to tilt towards the ground, as can be seen in the solid line in Fig. 6b. The distances were based on a bird's-eye view of the heat flux contours or flame length, not the curved flame length (i.e., the horizontal (x) distance to each heat flux contour shown by the blue-circles in the lower-left (x-z projection) of Fig. 6b).

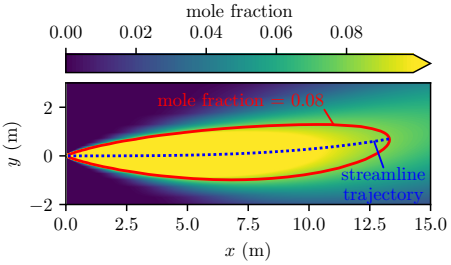

(a) Unignited dispersion.

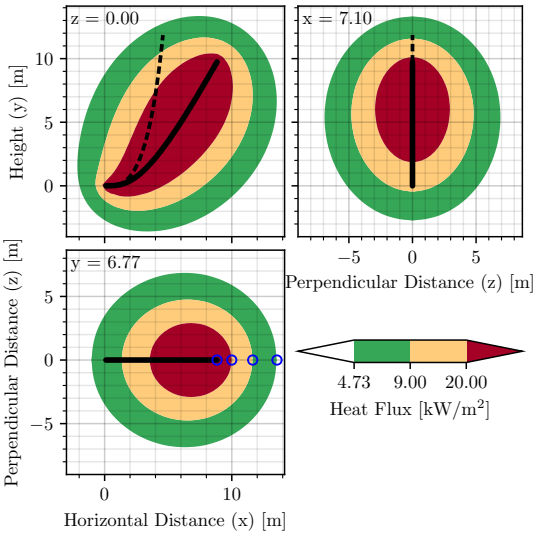

(b) Flame with dashed line showing trajectory without 5 m/s cross-wind and solid line showing trajectory with 5 m/s wind. Blue circles representing 'bird's-eye' distances to flame length and heat flux.

Figure 6. Example dispersion and flame calculations for a release of 414 kPa saturated liquid through an 8.5 mm diameter orifice (8.5 mm is the diameter for 5% of the flow area of a 38.1 mm inside diameter pipe).

As mentioned in Section 3.4, the model described by Jallais et al. [18] was used to calculate the overpressure, and similar to the flame, the bird's-eye distance to a given overpressure contour was calculated.

Calculations for each of the three groups are shown in Fig. 7. For group 1, it can be seen in Fig. 7a that the setback distance is driven by the streamline distance to the 8 vol-% mole fraction distance. This distance is further than both the distance to 6.9 kPa overpressure or 4.732 kW/m^2 heat flux. Figure 7b shows that the group 2 distance is driven by the 9 kW/m^2 heat flux criteria rather than the 13.8 kPa overpressure criteria. For group 3, Fig. 7c demonstrates that the 20 kW/m^2 heat flux criteria is longer than the visible flame length or the peak overpressure of 20.7 kPa. As would be expected, as the pipe size increases, the separation distance increases. The pressure also has a small influence on the distance, with the highest pressure tanks having the largest distance. However, lowering the tank pressure has much less of an effect than reducing the pipe size of a system.

Two tables are given in the 2023 edition of NFPA 2 [1], one for a typical liquid hydrogen system with a pipe inner diameter of 38.1 mm (1.5 in), and another where variations on pipe inner diameter and pressure are shown. The table with variations on pipe inner diameter and pressure is reproduced here in Table 3, with the typical pipe size highlighted with the bold values. The tables contain the same values as the thick solid lines in Fig. 7. Users of the tables in NFPA 2 can either read directly from the tables, interpolate values based on the tables, or use the equations given in Table 3.

Figure 8 graphically compares the previous bulk liquid separation distances to the current separation distances. For group 1, many system configurations with typical 38.1 mm inner diameter piping will require separation distances that are around 5% smaller than previous separation distances from lot lines and ignition sources, and nearly 40% smaller than the previous distances from air intakes and wall openings. The chart once again demonstrates that the pressure has a small effect on the distance while the pipe inner diameter has a larger effect. Even for 50.8 mm diameter piping, the separation distance remains below the previous distance of 22.9 m for air

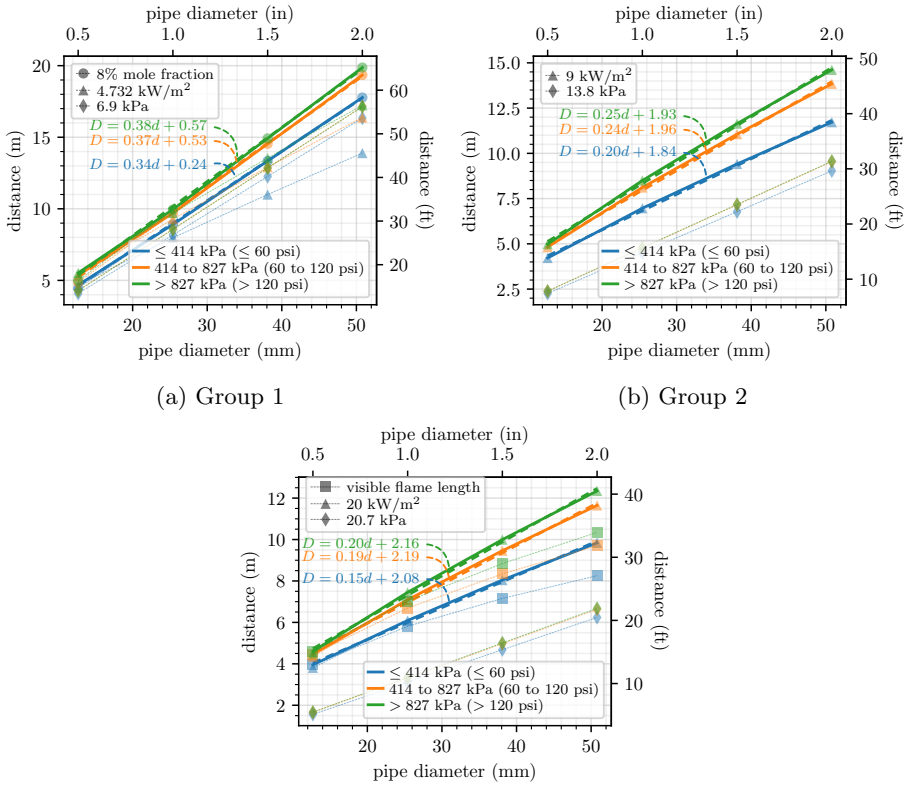

(a) Group 1

(b) Group 2

(c) Group 3

Figure 7. Setback distances for each of the three groups showing all criteria with the symbols and thin dashed lines as well as the maximum distance of the criteria shown by the thick solid lines, and a linear fit to the maximum shown by the thick thick dashed line.

Table 3. Minimum distance from outdoor bulk liquefied hydrogen systems to exposure by maximum inner diameter. The row with boldface is the typical diameter. For exposures within each group, the reader is directed to Table 1.

MAWP (gauge)		< 60 psi < 414 kPa						61 to 120 psi 415 to 827 kPa						121 to 173 psi 828 to 1200 kPa					
Exposures		Group 1		Group 2		Group 3		Group 1		Group 2		Group 3		Group 1		Group 2		Group 3	
Internal Pipe Diam↓/Eqn* →		$0.34d +$ 0.24		$0.20d +$ 1.84		$0.15d +$ 20.8		$0.37d +$ 0.53		$0.24d +$ 1.96		$0.19d +$ 2.19		$0.38d +$ 0.57		$0.25d +$ 1.93		$0.20d +$ 2.16	
in	mm	m	ft	m	ft	m	ft	m	ft	m	ft	m	ft	m	ft	m	ft	m	ft
0.5	12.7	4.7	15	4.2	14	4.0	13	5.4	18	4.8	16	4.5	15	5.5	18	5.0	16	4.6	15
1	25.4	8.9	29	7.0	23	6.1	20	9.7	32	8.2	27	7.1	23	10.0	33	8.5	28	7.5	25
1.5	**38.1**	**13.3**	**44**	**9.5**	**31**	**8.1**	**26**	**14.5**	**48**	**11.1**	**37**	**9.5**	**31**	**14.9**	**49**	**11.7**	**38**	**10.0**	**33**
2	50.8	17.8	58	11.8	39	9.9	32	19.3	63	13.9	46	11.7	38	19.9	65	14.7	48	12.4	41

* Fitted equation yields distance in meters using inner diameter, d, in mm.

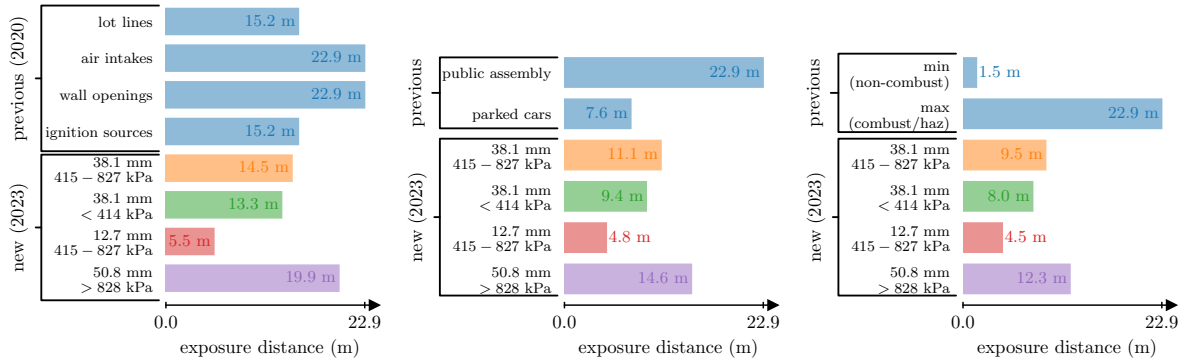

(a) Group 1 (b) Group 2 (c) Group 3

Figure 8. Bar charts showing the previous bulk liquid separation distances from NFPA 2 in blue and the 2023 separation distances for several system configurations.

intakes and wall openings. For group 2 with typical system piping of 38.1 mm, the separation distance to parked cars increases by 45%, but the distance to public assembly areas decreases by over 50%. The previous group 3 separation distances varied quite widely, from 1.5 m all the way to 22.9 m. Updated distances are much larger than the previous minimum distance, but shorter than the maximum distances.

Language in the 2023 edition of NFPA 2 also remains for distance reduction due to fire barrier walls. Group 3 distances can be reduced to 0 m, and groups 1 and 2 can be reduced by 50% by installing a fire-barrier wall blocking the line-of-site between any potential leak points and exposures. Language also remains enabling reduction of separation distances by 2/3 for vacuum insulated portions of the liquid hydrogen system. The updated distances that are a function of pipe size and pressure gives flexibility to liquid hydrogen infrastructure designers relative to the previous distances that were only based on storage volume.

4.0 SUMMARY AND CONCLUSIONS

The calculations that led to the updated separation distances between different exposures and bulk liquid hydrogen systems in the 2023 of NFPA 2 [1] are documented. The physics models in HyRAM+ version 4.1.1 were compared to literature data for liquid hydrogen flow through an orifice, unignited dispersion, radiation from flames, and the overpressure from the ignition of an unconfined plume. The algorithm for the homogeneous equilibrium model (HEM) for flow through an orifice was updated for version 4.1 of HyRAM+ to search for a maximum mass flux rather than rely on the uncertain 2-phase speed of sound calculation. For liquid hydrogen flows, this implementation agrees with other model predictions using a HEM. The flow rates predicted by the HEM tend to be equal to or larger than those measured experimentally. Notably the analysis did not account for pressure drop in the piping system due to friction. Modeling results for unignited dispersion from a liquid hydrogen source was compared to two data sets. The influence of wind was clear in the data; even neglecting this effect in the model, the calculated streamline distance to an 8% mole fraction was close to or (conservatively) slightly longer than the distances observed in the experiments. Only a single set of heat-flux data from a liquid hydrogen flame was identified in the literature and compared to the HyRAM+ model. Similar to the unignited concentrations, variability in the wind was evident in the data, but the birds-eye-view distances to different heat fluxes were conservatively predicted. Finally, the unconfined overpressure model was also compared to a single set of liquid hydrogen experiments. The overpressures were greatly overpredicted by the model (i.e. conservatively predicted). In short, the separation distances calculated by HyRAM+ result in accurate or conservative predictions, albeit with limited liquid hydrogen data for validation.

In separate work, Ehrhart et al. [4, 5] detail a risk-basis for a 5% by area characteristic leak size from a liquid hydrogen system. The HyRAM+ toolkit was exercised using this leak size to develop separation distances for three different groups of exposures that are based on the maximum allowable working pressure and the maximum pipe size of the liquid hydrogen system. While there were different distances for each exposure in previous editions of NFPA 2, separation distances to exposures that are now in group 1 tend to decrease relative to their previous values for a typical system. Some of the distances to exposures in group 2 increase while others decrease. Many of the separation distances to exposures in group 3 increase (although some decrease), but it should be noted that these distances can be reduced to 0 m with a fire barrier wall in between the liquid hydrogen system and the group 3 exposure.

Additional data for liquid hydrogen systems should be used in the future to further validate and/or improve the models for liquid hydrogen. Data is needed supporting the reduction credits due to fire barrier walls specific to liquid hydrogen systems (as these reduction credits are currently based on assessments of gaseous hydrogen systems). Quantitative risk assessment could be used to assess the reduction credit that remains for vacuum jacketed insulation. While the small leak size used in these consequence-based separation distance calculations will likely result in hydrogen vaporizing before interacting with surfaces, pooling and vaporization models are needed so that larger leaks can properly be accounted for in quantitative risk assessments or when simulating specific scenarios. A safety basis for larger bulk liquid hydrogen systems is also needed, as the current guidance is only for systems up to 280,000 l, which has been the maximum system size for bulk liquid hydrogen storage for using the setback distance tables (and not performing a system specific hazard analysis) in previous editions of NFPA 2. Larger systems have the potential to have long duration leaks that could have increasing hazards over time and/or larger pipe sizes.

5.0 ACKNOWLEDGMENTS

This work was supported by the Department of Energy Office of Energy Efficiency and Renewable Energy Hydrogen and Fuel Cell Technologies Office, as part of the Safety Codes and Standards program under the direction of Laura Hill. The authors appreciate the entire NFPA 2 storage task group for helpful comments, discussion and feedback as this analysis was being performed. Several members of the task group: Dave Farese and Derek Miller from Air Products and Tom Drube, Mukesh Trivedi, and John Anicello from Chart Industries provided critically important input, direction, discussion and feedback. Sandia National Laboratories is a multi-mission laboratory managed and operated by National Technology and Engineering Solutions of Sandia LLC, a wholly owned subsidiary of Honeywell International Inc. for the U.S. Department of Energy's National Nuclear Security Administration under contract DE-NA0003525. This paper describes objective technical results and analysis. Any subjective views or opinions that might be expressed in the paper do not necessarily represent the views of the U.S. Department of Energy or the United States Government.

REFERENCES

[1] NFPA 2, Hydrogen Technologies Code, National Fire Protection Association (2023).
[2] J. LaChance, Analyses to support development of risk-informed separation distances for hydrogen codes and standards, Tech. Rep. SAND2009-0874, Sandia National Laboratories (Mar. 2009).
[3] J. LaChance, Risk-informed separation distances for hydrogen refueling stations, international journal of hydrogen energy 34 (14) (2009) 5838–5845.
[4] B. D. Ehrhart, B. B. Schroeder, E. S. Hecht, Risk sensitivity study as the basis for risk-informed consequence-based setback distances for liquid hydrogen storage systems, in: 2023 International Conference on Hydrogen Safety, 2023.
[5] B. D. Ehrhart, E. S. Hecht, B. B. Schroeder, Technical justifications for liquid hydrogen exposure distances, Tech. Rep. SAND2023-12548, Sandia National Laboratories (Feb. 2023).
[6] K. Groth, G. W. Walkup, B. D. Ehrhart, A. B. Muna, M. L. Blaylock, E. Hecht, I. Ekoto, J. T. Reynolds, C. Sims, E. Carrier, B. Schroeder, HyRAM+ (hydrogen plus other alternative fuels risk assessment models) v.4.1.1, software, publically available repository at https://github.com/sandialabs/hyram.

[7] E. S. Hecht, B. D. Ehrhart, Hydrogen plus other alternative fuels risk assessment models (HyRAM+) version 4.1: Technical reference manual, Tech. Rep. SAND2022-5649, Sandia National Laboratories (Apr. 2022).
[8] B. Ehrhart, E. Hecht, J. Mohmand, Validation and comparison of hyram physics models, Tech. Rep. SAND2021-5811, Sandia National Laboratories (May 2021).
[9] Q. Guo, E. S. Hecht, M. L. Blaylock, J. G. Shum, C. Jordan, Physics model validation of propane and methane for hydrogen plus other alternative fuels risk assessment models (HyRAM+), Process Safety and Environmental Protection 173 (2023) 22–38.
[10] M. Royle, D. Willoughby, Releases of unignited liquid hydrogen, Tech. Rep. RR986, Health and Safety Executive, United Kingdom (2014).
[11] K. Lyons, S. Coldrick, G. Atkinson, Summary of experiment series e3.5 (rainout) results, Tech. rep., available at https://hysafe.info/wp-content/uploads/sites/3/2020/08/PRESLHY_D3.6_Summary_of_Rainout_Experiments_V1.20.pdf (2020).
[12] M. Huescar, A. Halford, J. Stene, Liquid hydrogen safety data report: Outdoor leakage study, Tech. Rep. 853182, Rev 2, DNV-GL (2020).
[13] K. B. Yüceil, M. V. Ötügen, Scaling parameters for underexpanded supersonic jets, Physics of Fluids 14 (12) (2002) 4206–4215.
[14] J. Grune, K. Sempert, M. Kuznetsov, T. Jordan, Hydrogen jet structure in presence of forced co-, counter- and cross-flow ventilation, in: 2023 International Conference on Hydrogen Safety, 2023.
[15] J. Grune, K. Sempert, M. Kuznetsov, T. Jordan, Hydrogen jet structure in presence of forced co-, counter- and cross-flow ventilation, in: Proceedings from the International Conference on Hydrogen Safety, 2021.
[16] W. Houf, R. Schefer, Predicting radiative heat fluxes and flammability envelopes from unintended releases of hydrogen, International Journal of Hydrogen Energy 32 (1) (2007) 136–151.
[17] I. W. Ekoto, A. J. Ruggles, L. Creitz, J. Li, Updated jet flame radiation modeling with buoyancy corrections, international journal of hydrogen energy 39 (35) (2014) 20570–20577.
[18] S. Jallais, E. Vyazmina, D. Miller, J. K. Thomas, Hydrogen jet vapor cloud explosion: a model for predicting blast size and application to risk assessment, Process safety progress 37 (3) (2018) 397–410.